Bosonization in the Presence of Confinement:

Calculation of the Nucleon-Nucleon Interaction

Shun-fu Gao, L.S. Celenza, C.M. Shakin[*],

Wei-Dong Sun, and J. Szweda

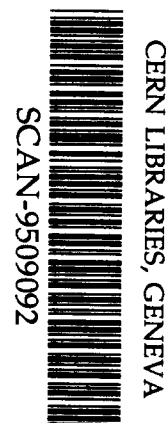Department of Physics and Center for Nuclear Theory

Brooklyn College of the City University of New York

Brooklyn, New York 11210

(August, 1995)

[*] e-mail: CASBC@CUNYVM.CUNY.EDU

Abstract

We describe an extended version of the Nambu−Jona-Lasinio (NJL) model that includes a description of confinement. It is necessary to incorporate some description of confinement in order to discuss the properties of the sigma, rho and omega mesons in the NJL model. These mesons, in addition to the pion, are the minimum needed to describe the salient features of the nucleon-nucleon interaction. In previous work we considered the relation between the bosonized NJL model and the one-boson-exchange (OBE) model of the nucleon-nucleon force. Most of our attention was given to pion and sigma exchange. We provide a review of that work and extend our discussion to a consideration of rho and omega exchange. We also present a more detailed discussion of the bosonization procedure. Our results depend upon the strength of the confining interaction. Once that is fixed, we obtain good values for the omega-nucleon coupling constant, $G_{\omega NN}$, and for the tensor coupling constant, f_ρ, in the rho-nucleon interaction. (One limitation of the present version of the model is that the ratio $f_\rho/g_\rho = 3.70$, instead of the empirical value of $f_\rho/g_\rho \simeq 6.1$.) If we consider nucleon-nucleon scattering for relatively small momentum transfer, we obtain good results for the processes of sigma, pion, rho, and omega exchange. Remarkably, the description of pion exchange is very accurate up to $q^2 \sim -2$ GeV^2. That is, the microscopic model reproduces the pion-exchange amplitude of the boson-exchange model over a broad range of momentum transfer when we use a pseudoscalar-isovector form factor of the nucleon obtained in a recent QCD lattice simulation. In the other channels (σ, ρ, ω), the nucleon form factors we calculate are too "soft" to fit the OBE amplitudes away from $q^2 \simeq 0$. Further work is needed to obtain good fits to the amplitudes for σ, ρ, and ω exchange for large momentum transfer, although the OBE amplitudes are well reproduced in the case of scattering at small momentum transfer ($|q^2| \leq 0.1$ GeV^2).

I. Introduction

It is useful to review some aspects of the NJL model [1] and our extension of that model to include a description of confinement [2-4]. The Lagrangian of our model is

$$\mathcal{L}(x) = \bar{q}(i\partial - m_q^0)q + \frac{G_S}{2}[(\bar{q}q)^2 + (\bar{q}i\gamma_5\vec{\tau}q)^2]$$
$$- \frac{G_\rho}{2}[(\bar{q}\gamma^\mu\vec{\tau}q)^2 + (\bar{q}\gamma_5\gamma_\mu\vec{\tau}q)^2] \qquad (1.1)$$
$$- \frac{G_\omega}{2}(\bar{q}\gamma^\mu q)^2 + \mathcal{L}_{conf}(x) \quad ,$$

where we see that there are three coupling constants to be fixed in addition to the current quark mass m_q^0. $\mathcal{L}_{conf}(x)$ introduces two constants, κ and μ, where κ is essentially the string tension and μ is a parameter introduced to simplify our momentum-space calculations [4]. More precisely, the confinement Lagrangian serves to introduce a potential between the quark and antiquark of the form $V^C(r) = \kappa r e^{-\mu r}$ [2,3]. Typically, we expect values of $\kappa \simeq 0.2$ GeV^2. (Also, we fix μ at 0.050 GeV to soften the momentum-space singularities of V^C.) We have fixed m_q^0 and G_S in an earlier work [5]. The choice of G_S is also related to the choice of the momentum-space cutoff needed in the NJL model. For example, for calculations made in a Euclidean momentum space, we choose $\Lambda_E = 1.0$ GeV. (That choice corresponds to a Minkowski-space cutoff for the magnitude of the various three-momenta in the loop integrals of the model of $\Lambda_3 = 0.702$ GeV.) For example, if $\Lambda_E = 1.0$ GeV, $m_q^0 = 5.5$ MeV, and $G_S = 7.91$ GeV^{-2}, we find the constituent quark mass to be $m_q = 262$ MeV and the pion mass $m_\pi = 138$ MeV. That choice of the parameters also yields satisfactory values for the pion decay constant, f_π, and the vacuum quark condensates $<0|\bar{u}u|0>$ and $<0|\bar{d}d|0>$ [5].

(In this work our notation is such that $\bar{q}q = \bar{u}u + \bar{d}d$, which differs from the conventional notation used in the discussion of QCD sum rules, where $<0|\bar{q}q|0>$ is either $<0|\bar{u}u|0>$ or $<0|\bar{d}d|0>$.)

The analysis proceeds by introducing fundamental quark-loop integrals for the pion and sigma channels [2,3],

$$J_P(q^2) = i n_c n_f \text{Tr} \int \frac{d^4p}{(2\pi)^4} \left[i\gamma_5 S_F \left(p + \frac{q}{2} \right) i\gamma_5 S_F \left(p - \frac{q}{2} \right) \right] \quad , \tag{1.2}$$

and

$$J_S(q^2) = n_c n_f \text{Tr} i \int \frac{d^4p}{(2\pi)^4} S_F \left(p + \frac{q}{2} \right) S_F \left(p - \frac{q}{2} \right) \quad . \tag{1.3}$$

[See Fig. 1.] The corresponding T matrices are

$$T_P = - \frac{G_S}{1 - G_S J_P(q^2)} \quad , \tag{1.4}$$

and

$$T_S = - \frac{G_S}{1 - G_S J_S(q^2)} \quad . \tag{1.5}$$

Here we have suppressed reference to the Dirac matrices and isospin operators that act in the quark-antiquark channels. The pion mass is zero if $m_q^0 = 0$. Otherwise, the pion mass is obtained from the relation

- 4 -

$$1 - G_S J_P(m_\pi^2) = 0 \quad . \tag{1.6}$$

The function $J_P(q^2)$ is shown in Fig. 2, where we have put $q^2 = t$.

When we turn to the sigma meson, we find the solution of $1 - G_S J_S(m_\sigma^2) = 0$ to lie in the $q\bar{q}$ continuum which starts at $q^2 = 4m_q^2$. That suggests that we need a model of confinement [2]. The model we use is described in Figs. 1 and 3 and their captions [2,3]. There we see that $q\bar{q}$ rescattering via the confinement potential, V^C, leads to the replacement of $J_S(q^2)$ by $\hat{J}_S(q^2)$. Note that, while $J_S(q^2)$ is complex for $q^2 > 4m_q^2$, $\hat{J}_S(q^2)$ is real. That is, the confinement vertex of Fig. 3, which is introduced to define $\hat{J}_S(q^2)$, removes the unphysical $q\bar{q}$ cut in $J_S(q^2)$. (See Fig. 1.)

It is also important to consider the amplitudes for $q + \bar{q} \to \pi + \pi$. To take those amplitudes into account we introduce $K_S(q^2)$ shown in Fig. 1. Consideration of confinement replaces $K_S(q^2)$ by $\hat{K}_S(q^2)$. The latter function has a (physical) cut for $q^2 > 4m_\pi^2$; the $q\bar{q}$ cuts for $q^2 > 4m_q^2$ are again removed by the confinement vertex functions. With the introduction of $\hat{K}_S(q^2)$, the T matrix of Eq. (1.5) becomes

$$\hat{T}_S(q^2) = -\frac{G_S}{1 - G_S[\hat{J}_S(q^2) + \hat{K}_S(q^2)]} \quad , \tag{1.7}$$

which only has a physical cut starting at $q^2 = 4m_\pi^2$, since $\hat{J}_S(q^2)$ is real, as noted above.

While the theory without confinement leads to $m_\sigma^2 = 4m_q^2 + m_\pi^2$ in the simplest bosonization analysis [6], it is known that there is no low-mass sigma ($m_\sigma \simeq 540$ MeV) to be found in the data tables. To see how the introduction of confinement resolves that problem we may refer to Fig. 4, where we show $\hat{J}_S(t)$ for $t = q^2 > 0$. The values for $t < 0$ represent

$J_S(t)$ calculated in a Euclidean momentum space with $\Lambda_E = 1.0$ GeV. Note that, $J_S(t) \simeq \hat{J}_S(t)$ for $t < 0$ and we do not distinguish between these functions in that region. For $t > 0$, $\hat{J}_S(t)$ is calculated in Minkowski momentum space with $\Lambda_3 = 0.702$ GeV and $\kappa = 0.20$ GeV^2. The dashed curve shows $J_S(t)$ for $t > 0$. It is useful to consider a horizontal line that could be drawn with ordinate equal to $1/G_S$, since the solution of

$$\frac{1}{G_S} - J_S(m_\sigma^2) = 0 \quad , \tag{1.8}$$

or

$$\frac{1}{G_S} - \hat{J}_S(m_\sigma^2) = 0 \quad , \tag{1.9}$$

yields the sigma mass. Note that we may generalize Eq. (1.9) to read

$$\frac{1}{G_S} - \left[\hat{J}_S(m_\sigma^2) + \mathrm{Re}\,\hat{K}_S(m_\sigma^2)\right] = 0 \quad . \tag{1.10}$$

The solution of Eq. (1.9), or Eq. (1.10), yields $m_\sigma \simeq 900$ MeV, which takes the sigma out of the low-energy regime. In Fig. 5, we show $\hat{J}_S(t)$ for $t > 0$ and for various values of κ. It may be seen that the larger values of κ will move the sigma still higher in energy for fixed G_S, as it to be expected when a repulsive potential of increasing strength is introduced. We remark that use of Eq. (1.10) yields slightly higher values for m_σ, since $\mathrm{Re}\,\hat{K}_S(q^2)$ is negative for $q^2 > 0.25$ GeV^2, while $\hat{J}_S(q^2)$ is everywhere positive. However, $\mathrm{Re}\,\hat{K}_S(q^2)$ is small in this case and may be neglected. (For example, for $q^2 = 0.8$ GeV^2, $\mathrm{Re}\,\hat{K}_S(q^2) = -0.006$ GeV^2 while $\hat{J}_S(q^2) \simeq 0.12$ GeV^2, if $\kappa = 0.20$ GeV^2.)

II. Bosonization of the Extended NJL Model: Scalar-Isoscalar Mode

We will use a generalized version of the momentum-space bosonization scheme introduced in Ref. [6]. There it is shown that one may write for the scalar-isoscalar channel,

$$-\frac{G_S}{1 - G_S J_S(q^2)} = \frac{g^2_{\sigma qq}(q^2)}{q^2 - m^2_\sigma(q^2)} \quad . \tag{2.1}$$

Explicit expressions are given for $J_S(q^2)$ and the momentum-dependent coupling constant and mass in Ref. [6].

In our extended version of the NJL model, we replace $J_S(q^2)$ by $\hat{J}_S(q^2)$ and also include $\hat{K}_S(q^2)$ in the denominator of the T matrix in some cases. It is then useful to write $\hat{J}_S(q^2)$ as

$$\hat{J}_S(q^2) = s_1 - \frac{s_2}{q^2 - \tilde{m}^2_\sigma} \tag{2.2}$$

where s_1, s_2 and $\tilde{m}_\sigma$ are constants. (This form may be used for spacelike values of q^2, even if we do not find a pole in $\hat{J}_S(q^2)$ for $q^2 > 0$.) We now write

$$\hat{T}_S(q^2) = -\frac{1}{G_S^{-1} - \hat{J}_S(q^2)} \quad , \tag{2.3}$$

$$= -\frac{\left[\dfrac{q^2 - \tilde{m}^2_\sigma}{G_S^{-1} - s_1}\right]}{q^2 - \left[\tilde{m}^2_\sigma - \dfrac{s_2}{G_S^{-1} - s_1}\right]} \quad . \tag{2.4}$$

Therefore, we may put

$$m_\sigma^2 = \tilde{m}_\sigma^2 - \frac{s_2}{G_S^{-1} - s_1} \quad , \tag{2.5}$$

and also define a momentum-dependent coupling constant (with $q^2 < \tilde{m}_\sigma^2$),

$$g_{\sigma qq}^2(q^2) = \frac{\tilde{m}_\sigma^2 - q^2}{G_S^{-1} - s_1} \quad , \tag{2.6}$$

which arises naturally in this formalism. Note that we will define $g_{\sigma qq}^2 = g_{\sigma qq}^2(0)$, with

$$g_{\sigma qq}^2(0) = \frac{\tilde{m}_\sigma^2}{G_S^{-1} - s_1} \quad . \tag{2.7}$$

With the various definitions given above, we have

$$\hat{T}_S(q^2) = \frac{g_{\sigma qq}^2(q^2)}{q^2 - m_\sigma^2} \quad . \tag{2.8}$$

We also see that

$$\frac{1}{G_S^{-1} - \hat{J}_S(0)} = \frac{g_{\sigma qq}^2(0)}{m_\sigma^2} \quad , \tag{2.9}$$

which is a useful relation for obtaining $g_{\sigma qq}^2$ from knowledge of G_S and $\hat{J}_S(0)$.

The situation in the case of the scalar-isoscalar channel is quite subtle, since the choice of parameters depends on the physical situation. For example, our studies have shown that, for spacelike values of q^2 near $q^2 = 0$, the value of m_σ in Eq. (2.8) is 540 MeV and $g_{\sigma qq}(0) = 2.58$, in one case [5]. However, there is no pole in the T matrix for $q^2 = m_\sigma^2$, with $m_\sigma = 540$ MeV. For example, as we will see, for timelike q^2 we find a pole at $q^2 = m_\sigma^2$,

where $m_\sigma \simeq 900$ MeV, if $\kappa = 0.20$ GeV^2. One way to understand this point is to note that $J_S(q^2)$ and $\hat{J}_S(q^2)$ are quite similar for $q^2 < 0$, while these functions are quite different for timelike q^2. [See Fig. 4.] Note that the rapid rise of $J_S(q^2)$ for $q^2 > 0$ seen in Fig. 4 is due to the presence of a $q\bar{q}$ cut starting at $q^2 = 4m_q^2 = 0.275$ GeV^2. Beyond that point $J_S(q^2)$ is complex. On the other hand, $\hat{J}_S(q^2)$ is everywhere real and a rapid rise in the value of that function could signal the presence of a bound state in the (linear) confining potential.

As a specific example, relevant to the <u>spacelike</u> region, consider the parameters $\bar{m}_\sigma^2 = 0.520$ GeV^2, $s_1 = 0.0479$ GeV^2 and $s_2 = 0.0178$ GeV^4. These values yield $m_\sigma = 0.540$ GeV, $g_{\sigma qq}(0) = 2.58$ and $\hat{J}_S(0) = 0.0821$ GeV^2. This parametrization describes the behavior of $\hat{J}_S(q^2)$ rather well for -0.3 GeV$^2 < q^2 < 0$; however, there is no pole at $\bar{m}_\sigma^2 = 0.520$ GeV^2 in the timelike region. (See Fig. 7 of Ref. [8].)

Note that, if we include $\hat{K}_S(q^2)$ in our considerations and use $\kappa = 0.22$ GeV^2, we find $\hat{J}_S(0) + \hat{K}_S(0) = 0.0917$ GeV^2. Therefore, using $\hat{J}_S(0) + \hat{K}_S(0)$ instead of $\hat{J}_S(0)$ in Eq. (2.9), we find $g_{\sigma qq}(0) = 2.90$, if we again use $G_S = 7.91$ GeV^{-2} and $m_\sigma = 0.540$ GeV. This modification serves to enhance the magnitude of the T matrix at $q^2 = 0$ by about 27 percent relative to the result obtained when we neglect $\hat{K}_S(q^2)$. (We remark that an easy way to obtain Re $\hat{K}_S(q^2)$ is to calculate Im $\hat{K}_S(q^2)$ and then obtain Re $\hat{K}_S(q^2)$ by use of a dispersion relation [2].)

The rather complex situation that exists in the case of the sigma meson is greatly simplified when we consider the omega and rho mesons, since a single parametrization of the form of Eq. (2.2) may be used both in the spacelike and the timelike regions.

III. Bosonization for the Omega Meson

It is useful to divide the omega propagator and T matrix into transverse and longitudinal parts [3]. For example, we may write

$$\frac{[g^{\mu\nu} - q^{\mu}q^{\nu}/m_{\omega}^2]}{q^2 - m_{\omega}^2} = \frac{[g^{\mu\nu} - q^{\mu}q^{\nu}/q^2]}{q^2 - m_{\omega}^2} - \frac{q^{\mu}q^{\nu}}{q^2 m_{\omega}^2} \quad . \tag{3.1}$$

One may also define the function $\hat{J}_{(\omega)}(q^2)$, related to a tensor $\hat{J}^{\mu\nu}_{(\omega)}(q^2)$. Here,

$$\hat{J}^{\mu\nu}_{(\omega)}(q^2) = -\left[g^{\mu\nu} - \frac{q^{\mu}q^{\nu}}{q^2}\right]\hat{J}_{(\omega)}(q^2) \quad , \tag{3.2}$$

where [3]

$$-i\hat{J}^{\mu\nu}_{(\omega)}(q^2) = (-1)n_c n_f \mathrm{Tr} \int \frac{d^4k}{(2\pi)^4}\left[iS_F(q/2 + k)\Gamma^{\mu}(q, k)\, iS_F(-q/2 + k)\hat{\gamma}^{\nu}\right] \quad . \tag{3.3}$$

In this case $\Gamma^{\mu}(q, k)$ contains the vertex for the confining field and

$$\hat{\gamma}^{\nu} \equiv \gamma^{\nu} - \slashed{q}q^{\nu}/q^2 \quad . \tag{3.4}$$

Note that $q_{\mu}\hat{J}^{\mu\nu}_{(\omega)}(q^2) = \hat{J}^{\mu\nu}_{(\omega)}(q^2)q_{\nu} = 0$ in accord with Eq. (3.2), since $q_{\mu}\Gamma^{\mu} = q_{\mu}\hat{\gamma}^{\mu} = 0$ [3].

In Fig. 6 we show $\hat{J}_{(\omega)}(t)$ for $\kappa = 0.16$ GeV^2, $\kappa = 0.22$ GeV^2, and $\kappa = 0.28$ GeV^2. A vertical line drawn at $t = m_{\omega}^2$ intersects each of these curves at a point. The ordinate of that point then yields a value for $1/G_{\omega}$, since the (transverse) T matrix may be written

$$\hat{T}^{\mu\nu}_{(\omega)} = -[g^{\mu\nu} - q^{\mu}q^{\nu}/q^2]\hat{T}_{(\omega)}(q^2) \quad , \tag{3.5}$$

with

- 10 -

$$\hat{T}_{(\omega)}(q^2) = \frac{1}{\dfrac{1}{G_\omega} - \hat{J}_{(\omega)}(q^2)} \quad . \tag{3.6}$$

A particularly useful representation for $\hat{J}_{(\omega)}(q^2)$ that has a simple physical interpretation is given by

$$\hat{J}_{(\omega)}(q^2) = v_1 - \frac{v_2}{q^2 - \tilde{m}_\omega^2} \quad . \tag{3.7}$$

In terms of these parameters, we have

$$m_\omega^2 = \tilde{m}_\omega^2 - \frac{v_2}{G_\omega^{-1} - v_1} \tag{3.8}$$

and

$$g_{\omega qq}^2(0) = \frac{\tilde{m}_\omega^2}{G_\omega^{-1} - v_1} \quad . \tag{3.9}$$

For example, if $\kappa = 0.22$ GeV^2, we find that with $G_\omega = 7.86$ GeV^{-2}, $v_1 = 0.0284$ GeV^2, $v_2 = 0.0850$ GeV^4 and $\tilde{m}_\omega^2 = 1.476$ GeV^2, we obtain an accurate representation of $\hat{J}_{(\omega)}(q^2)$ for $q^2 > 0$. This result may be understood by interpreting $\tilde{m}_\omega$ as the mass of a bound state in the linear confining potential. (Note that $\tilde{m}_\omega$ is obtained in the absence of the short-range attraction parametrized by G_ω.) The introduction of the short-range interaction then moves the bound state down to $m_\omega = 0.783$ GeV. As noted above, this situation is much simpler than that in the scalar-isoscalar channel, since m_ω of Eq. (3.8) is equal to 0.783 GeV in both the timelike and spacelike domains of q^2.

At this point in our discussion, we have $\hat{J}_{(\omega)}(0) \neq 0$. That result would lead to the generation of a mass for the photon. To avoid that we may make a subtraction, replacing

$\hat{J}_{(\omega)}(q^2)$ by $\hat{J}_{(\omega)}(q^2) - \hat{J}_{(\omega)}(0)$. It is readily seen that, if we simultaneously replace G_ω^{-1} by $G_\omega^{-1} - J_\omega(0)$, there is no change in the quark T matrix, so that the values of m_ω and $g_{\omega qq}$ are unchanged by the subtraction.

IV. Bosonization for the Rho Meson

Here, the new feature relative to the previous section is the importance of a tensor that describes the coupling of $q\bar{q}$ states to the two-pion continuum [3],

$$\hat{K}_{(\rho)}^{\mu\nu}(q^2) = - \left[g^{\mu\nu} - \frac{q^\mu q^\nu}{q^2} \right] \hat{K}_{(\rho)}(q^2) \quad , \tag{4.1}$$

in addition to the tensor

$$\hat{J}_{(\rho)}^{\mu\nu}(q^2) = - \left[g^{\mu\nu} - \frac{q^\mu q^\nu}{q^2} \right] \hat{J}_{(\rho)}(q^2) \quad . \tag{4.2}$$

The (transverse) T matrix is of the form

$$\hat{T}_{(\rho)}^{\mu\nu}(q^2) = - \left[g^{\mu\nu} - \frac{q^\mu q^\nu}{q^2} \right] \hat{T}_{(\rho)}(q^2) \quad , \tag{4.3}$$

with

$$\hat{T}_{(\rho)}(q^2) = \frac{1}{G_\rho^{-1} - [\hat{J}_{(\rho)}(q^2) + \hat{K}_{(\rho)}(q^2)]} \quad . \tag{4.4}$$

Since m_ρ^2 is known, we find the appropriate value of G_ρ by solving the equation

$$\frac{1}{G_\rho} - [\hat{J}_{(\rho)}(m_\rho^2) + \text{Re} \, \hat{K}_{(\rho)}(m_\rho^2)] = 0 \quad . \tag{4.5}$$

- 12 -

Again, we may indicate how this solution appears in a graphical form. For example, in Fig. 7, with $t = q^2$, we show $\hat{J}_{(\rho)}(q^2) + \text{Re}\,\hat{K}_{(\rho)}(q^2)$ for various κ. (Note that $\hat{J}_{(\rho)}(q^2) = \hat{J}_{(\omega)}(q^2)$.) Figure 8 shows $\text{Re}\,K_{(\rho)}(t)$ for various value of κ. Since we have fixed $\kappa = 0.22$ GeV^2 in our study of the omega meson, we use that value here and find that $G_\rho = 7.12$ GeV^{-2} yields a rho meson with $m_\rho = 0.770$ GeV.

In this case, we put

$$\hat{J}_{(\rho)}(q^2) + \text{Re}\,\hat{K}_{(\rho)}(q^2) = r_1 - \frac{r_2}{q^2 - \tilde{m}_\rho^2} \quad , \tag{4.6}$$

so that

$$m_\rho^2 = \tilde{m}_\rho^2 - \frac{r_2}{G_\rho^{-1} - r_1} \quad , \tag{4.7}$$

and

$$g_{\rho qq}^2(q^2) = \frac{\tilde{m}_\rho^2 - q^2}{G_\rho^{-1} - r_1} \quad , \tag{4.8}$$

in analogy to what was done for the omega meson. Again, $g_{\rho qq}^2 = g_{\rho qq}^2(0)$, with

$$g_{\rho qq}^2(0) = \frac{\tilde{m}_\rho^2}{G_\rho^{-1} - r_1} \quad . \tag{4.9}$$

A good fit to $\hat{J}_{(\rho)}(q^2) + \text{Re}\,\hat{K}_{(\rho)}(q^2)$ for $q^2 \geq 0$ is obtained if $r_1 = 0.0304$ GeV^2, $r_2 = 0.0968$ GeV^4 and $\tilde{m}_\rho^2 = 1.476$ GeV^2. (As noted above, $G_\rho = 7.12$ GeV^{-2}.)

V. The Nucleon-Nucleon Interaction in the OBE and NJL Models

In Fig. 9a we represent meson exchange in the OBE model on the left-hand side of the figure. There, the open circles are the form factors of the OBE model that are of the (monopole) form

$$F_i^{OBE}(t) = \left[\frac{\Lambda_i^2 - m_i^2}{\Lambda_i^2 - t} \right] \tag{5.1}$$

for a meson of mass m_i and OBE cut-off Λ_i. On the right-hand side of Fig. 9a we represent the interaction in terms of the quark-quark interaction, T. We do not consider all possible diagrams, but isolate those diagrams that are of leading order in $1/n_c$ counting [8]. The interaction in that case may be expressed in terms of the functions, $\hat{J}(q^2)$ and $\hat{K}(q^2)$, for the various mesons. For example, in Fig. 9b we show those interactions that lead to the use of

$$t_{qq}^{(\sigma)}(t) = -\frac{G_S}{1 - G_S \hat{J}_S(t)} \tag{5.2}$$

in the case of sigma exchange. To keep in mind that we sum only the leading diagrams, we denoted the quark-quark T matrix as t_{qq} in Fig. 9c and in Eq. (5.2).

Pion Exchange

With reference to Fig. 9, we write a scattering amplitude for pion exchange in the OBE model as

$$f_\pi^{OBE}(t) = \frac{g_{\pi NN}^2}{4\pi} \left[\frac{\Lambda_\pi^2 - m_\pi^2}{\Lambda_\pi^2 - t} \right]^2 \frac{1}{t - m_\pi^2} \; , \tag{5.3}$$

- 14 -

$$= f_\pi^{OBE}(0) h_\pi^{OBE}(t) \quad . \tag{5.4}$$

In Eq. (5.3) we have included the form factors of the OBE model that appear at each pion-nucleon vertex. It is also useful to define

$$\frac{G_{\pi NN}^2}{4\pi} = \frac{g_{\pi NN}^2}{4\pi} \left[\frac{\Lambda_\pi^2 - m_\pi^2}{\Lambda_\pi^2} \right]^2 \quad , \tag{5.5}$$

with similar definitions for the sigma, rho and omega mesons. The amplitude corresponding to $f_\pi^{OBE}(t)$ in the NJL model is (see Fig. 9c),

$$f_\pi^{NJL}(t) = \frac{t_{qq}^{(\pi)}(t)}{4\pi} \left(\tilde{F}_\pi(t) \right)^2 \quad , \tag{5.6}$$

$$= f_\pi^{NJL}(0) h_\pi^{NJL}(t) \quad . \tag{5.7}$$

Here, $t_{qq}^{(\pi)}$ is the quark-quark scattering amplitude of the NJL model and $\tilde{F}_\pi(t)$ is a nucleon form factor defined such that

$$\tilde{F}_\pi(t) \bar{u}(\vec{p}+\vec{q}, s') i\gamma_5 u(\vec{p}, s) <t' | \vec{\tau} | t> \ = \ <\vec{p}+\vec{q}, s', t' | \bar{q}(0) i\gamma_5 \vec{\tau} q(0) | \vec{p}, s, t> \tag{5.8}$$

It is useful to introduce a monopole form for the nucleon form factor,

$$\tilde{F}_\pi(t) = \tilde{F}_\pi(0) \left[\frac{\lambda_\pi^2}{\lambda_\pi^2 - t} \right] \quad , \tag{5.9}$$

- 15 -

and note that in a recent lattice simulation of QCD it was found that $\lambda_\pi = 0.75 \pm 0.14$ GeV [9].

In a previous work [8] we saw that, with $\lambda_\pi = 0.8$ GeV, there was excellent agreement of the functions $h_\pi^{NJL}(t)$ and $h_\pi^{OBE}(t)$. [See Fig. 10.] Here, we also consider the magnitude of the amplitude in addition to the q^2 dependence, so that we have to provide a value for $\tilde{F}_\pi(0)$. In an earlier work, we found $\tilde{F}_\pi(0) = 4.78$, when we calculated the form factor $\tilde{F}_\pi(t)$ in a covariant soliton model of the nucleon [10]. Near $t \simeq 0$, we may put $t_{qq}^{(\pi)}(t) = g_{\pi qq}^2/(t - m_\pi^2)$, so that, in our model,

$$f_\pi^{NJL}(0) = -\frac{g_{\pi qq}^2}{4\pi} \frac{[\tilde{F}_\pi(0)]^2}{m_\pi^2} \quad , \tag{5.10}$$

$$= -676 \text{ GeV}^{-2} \quad , \tag{5.11}$$

where we have used $g_{\pi qq} = 2.68$ and $\tilde{F}_\pi(0) = 4.78$, as found in our earlier work [5,10]. Noting that $\Lambda_\pi = 1.3$ GeV and $g_{\pi NN}^2/4\pi = 14.4$ in typical OBE model calculations [7], we have

$$f_\pi^{OBE}(0) = -727 \text{ GeV}^{-2} \quad , \tag{5.12}$$

which is only 8 percent greater than $f_\pi^{NJL}(0)$ given in Eq. (5.11). Thus, we see that for pion exchange we fit both the value of $G_{\pi NN}\left(G_{\pi NN} = g_{\pi qq}\tilde{F}_\pi(0) = 12.8\right)$ and the q^2 dependence of the amplitude up to $-q^2 \simeq 2$ GeV^2. We ascribe this success to the fact that we were able to take a value for λ_π from the recent QCD calculation [9], since our calculation of $\tilde{F}_\pi(t)$ gave

- 16 -

a form factor that was too soft. For example, the quark wave function of Ref. [10] yields a dipole form for the form factor,

$$\tilde{F}_\pi(t) = \tilde{F}_\pi(0) \left[\frac{1}{1 - \dfrac{t}{0.36}} \right]^2 \, , \qquad (5.13)$$

where $\tilde{F}_\pi(0) = 4.78$ and t is in GeV^2 units. For a monopole fit, the effective vertex parameter would be about $\lambda_\pi = 0.43$ GeV, which may be compared to the result based upon the lattice simulation of QCD that gave $\lambda_\pi = 0.75 = \pm 0.14$ GeV [9]. (Recall that putting $\lambda_\pi = 0.80$ GeV in our analysis gave an excellent fit to the q^2 dependence of the OBE amplitudes, as shown in Fig. 10.)

Sigma Exchange

To study sigma exchange we need the nucleon form factor, $F_S(t)$, defined by the relation

$$F_S(t) u(\vec{p} + q, s') u(\vec{p}, s) \delta_{tt'} = < \vec{p} + \vec{q}, s', t' \,|\, \bar{q}(0) q(0) \,|\, \vec{p}, s, t > \quad . \qquad (5.14)$$

We may write

$$f_\sigma^{OBE}(t) = \frac{g_{\sigma NN}^2}{4\pi} \left[\frac{\Lambda_\sigma^2 - m_\sigma^2}{\Lambda_\sigma^2 - t} \right]^2 \frac{1}{t - m_\sigma^2} \, , \qquad (5.15)$$

$$= f_\sigma^{OBE}(0) \, h_\sigma^{OBE}(t) \quad , \qquad (5.16)$$

and

$$f_\sigma^{NJL}(t) = \frac{t_{qq}^{(\sigma)}(t)}{4\pi} [F_S(t)]^2 \quad . \qquad (5.17)$$

Now

$$f_\sigma^{OBE}(0) = - \frac{g_{\sigma NN}^2}{4\pi} \left[\frac{\Lambda_\sigma^2 - m_\sigma^2}{\Lambda_\sigma^2} \right]^2 \frac{1}{m_\sigma^2} \quad , \tag{5.18}$$

$$= - \frac{G_{\sigma NN}^2}{4\pi} \frac{1}{m_\sigma^2} \quad , \tag{5.19}$$

while

$$f_\sigma^{NJL}(0) = - \frac{g_{\sigma qq}^2}{4\pi} \frac{1}{m_\sigma^2} [F_S(0)]^2 \quad . \tag{5.20}$$

Thus, we would like to have

$$G_{\sigma NN} = g_{\sigma qq} F_S(0) \quad , \tag{5.21}$$

where the phenomenological value of $G_{\sigma NN}$ is in the range $9.31 \leq G_{\sigma NN} \leq 9.73$, if $\Lambda_\sigma = 2.0$ GeV, and $m_\sigma = 0.550$ GeV [7]. In a recent work, we calculated $F_S(0)$ and found that Eq. (5.21) was well satisfied [11]. Therefore, in addition to obtaining a satisfactory value for $G_{\pi NN}$, we also obtain a good value for $G_{\sigma NN}$ in our model. It is worth remarking that in the earlier work mentioned above, we had $F_S(0) = 1.94$ [10]. However, vertex corrections enhance that value by about 80 percent [11], so that Eq. (5.21) is satisfied when $g_{\sigma qq} = 2.58$ (obtained in Ref. [5]) is used.

Omega Exchange

In the simplest approximation, the omega has as its source the isoscalar current $j^\mu(x) = \bar{q}(x) \gamma^\mu q(x)$, which is six times the isoscalar electromagnetic current. We define two

- 18 -

form factors, $F_{10}^{(\omega)}(q^2)$ and $F_{20}^{(\omega)}(q^2)$, which are proportional to the isoscalar electromagnetic form factors of the nucleon

$$< \vec{p} + \vec{q}, s', t' \mid \bar{q}(0)\gamma^\mu q(0) \mid \vec{p}, s, t > = \delta_{tt'} \bar{u}(\vec{p} + \vec{q}, s')[\gamma^\mu F_{10}^{(\omega)}(q^2)$$
$$+ \frac{i\sigma^{\mu\nu}q_\nu}{2m_N} F_{20}^{(\omega)}(q^2)]u(\vec{p}, s) \quad . \tag{5.22}$$

Note that $F_{10}^{(\omega)}(0) = 3$ and that $F_{20}^{(\omega)}(q^2)$ is quite small and may be dropped.

Then, in analogy to Eqs. (5.15) and (5.17), we define

$$f_\omega^{OBE}(t) = -\frac{g_{\omega NN}^2}{4\pi}\left[\frac{\Lambda_\omega^2 - m_\omega^2}{\Lambda_\omega^2 - t}\right]^2 \frac{1}{t - m_\omega^2} \quad , \tag{5.23}$$

$$= f_\omega^{OBE}(0)\, h_\omega^{OBE}(t) \quad , \tag{5.24}$$

and

$$f_\omega^{NJL}(t) = \frac{t_{qq}^{(\omega)}(t)}{4\pi}[F_{10}^{(\omega)}(t)]^2 \quad . \tag{5.25}$$

Now

$$f_\omega^{OBE}(0) = \frac{g_{\omega NN}^2}{4\pi}\left[\frac{\Lambda_\omega^2 - m_\omega^2}{\Lambda_\omega^2}\right]^2 \frac{1}{m_\omega^2} \quad , \tag{5.26}$$

so that, if we set $f_\omega^{OBE}(0)$ equal to $f_\omega^{NJL}(0)$, we have

$$\frac{g_{\omega NN}^2}{4\pi} \left[\frac{\Lambda_\omega^2 - m_\omega^2}{\Lambda_\omega^2} \right]^2 = 9 \frac{g_{\omega qq}^2}{4\pi} \ . \tag{5.27}$$

This equation is used to define the theoretical value for $g_{\omega NN}$ in terms of $g_{\omega qq}$. In empirical OBE potentials [7] one has $g_{\omega NN}^2/4\pi = 20.0$, $\Lambda_\omega = 1.5$ GeV and $m_\omega = 0.783$ GeV. The bosonization scheme, in conjunction with Fig. 6 and Table 1, shows that, if we choose $\kappa = 0.22$ GeV^2, we have $g_{\omega qq}^2/4\pi = 1.19$. Then use of Eq. [5.27] yields $g_{\omega NN}^2/4\pi = 20.2$. Thus, Eq. (5.27) is well satisfied when $\kappa = 0.22$ GeV^2 and is satisfied to about 10 percent accuracy if $\kappa = 0.20$ GeV^2. (See Table 1.)

When we compare the q^2 dependence of $f_\omega^{OBE}(t)$ and $f_\omega^{NJL}(t)$, we find that, if we write

$$h_\omega^{NJL}(t) = \left[\frac{\lambda_\omega^2}{\lambda_\omega^2 - t} \right]^2 \frac{t_{qq}^{(\omega)}(t)}{t_{qq}^{(\omega)}(0)} \ , \tag{5.28}$$

we would need to put $\lambda_\omega = 0.93$ GeV to obtain a very good fit for $-q^2 \leq 2$ GeV^2 [8]. However, since the electromagnetic form factors of the nucleon are of the dipole form, for example,

$$G_E^P(t) = \frac{1}{\left[1 - \dfrac{t}{(0.84)^2} \right]^2} \ , \tag{5.29}$$

we again see that the effective value of λ_ω for a monopole form factor in our model is about 600 MeV, rather than the 930 MeV needed to fit $f_\omega^{OBE}(t)$ over a broad range of spacelike values of q^2.

Rho Exchange

In the simplest model of the rho-nucleon vertex, the rho has as its source the isovector current $\vec{j}^{\mu}(x) = \bar{q}(x)\gamma^{\mu}\vec{\tau}q(x)$, which may be related to the isovector electromagnetic current $j_{em}^{\mu}(x) = \bar{q}(x)\gamma^{\mu}\frac{\tau_3}{2}q(x)$. We again define two factors:

$$< \vec{p} + \vec{q}, s', t' \mid \vec{j}^{\mu}(0) \mid \vec{p}, s, t > \; = \; <t' \mid \vec{\tau} \mid t > \bar{u}(\vec{p} + \vec{q}, s')[\gamma^{\mu} F_{11}^{(\rho)}(q^2)$$

$$+ i\frac{\sigma^{\mu\nu}q_{\nu}}{2m_N} F_{21}^{(\rho)}(q^2)] \, u \, (\vec{p}, s) \quad , \tag{5.30}$$

with $F_{11}^{(\rho)}(0) = 1$ and $F_{21}^{(\rho)}(0) = 3.70$. Our strategy will be to assume that $F_{10}^{(\rho)}(q^2)$ and $F_{21}^{(\rho)}(q^2)$ have similar dependence on q^2, so that we may write $F_{21}^{(\rho)}(q^2) = 3.70\, F_{11}^{(\rho)}(q^2)$. With that in mind, we will concentrate on the first term on the right-hand side of Eq. (5.30). In this approximation, our study of rho exchange is similar to our study of omega exchange.

We define

$$f_{\rho}^{OBE}(t) \; = \; -\frac{g_{\rho NN}^2}{4\pi}\left[\frac{\Lambda_{\rho}^2 - m_{\rho}^2}{\Lambda_{\rho}^2 - t}\right]^2 \frac{1}{t - m_{\rho}^2} \quad , \tag{5.31}$$

$$= f_{\rho}^{OBE}(0)\, h_{\rho}^{OBE}(t) \quad , \tag{5.32}$$

and

$$f_{\rho}^{NJL}(t) \; = \; \frac{t_{qq}^{(\rho)}(t)}{4\pi}\, [F_{10}^{(\rho)}(t)]^2 \quad , \tag{5.33}$$

$$= f_\rho^{NJL}(0) h_\rho^{NJL}(t) \quad . \tag{5.34}$$

We may obtain a theoretical value for $g_{\rho NN}^2/4\pi$ by equating the amplitudes for $t = 0$,

$$\frac{g_{\rho NN}^2}{4\pi} \left[\frac{\Lambda_\rho^2 - m_\rho^2}{\Lambda_\rho^2} \right]^2 = \frac{g_{\rho qq}^2}{4\pi} \quad , \tag{5.35}$$

where we have used the fact that $F_{11}^{(\rho)}(0) = 1$. To obtain $g_{\rho NN}^2/4\pi$ we proceed as in the case

of the omega meson and use the formalism of Section IV. Since we have set $\kappa = 0.22$ GeV^2,

we need values of $\hat{J}_{(\rho)}(t) + \hat{K}_{(\rho)}(t)$ for that value of κ. Those values are exhibited in Fig. 7.

Requiring that $m_\rho = 0.770$ GeV, we obtain $G_\rho = 7.12$ GeV^{-2} from Eq. (4.5), and then use

$$\frac{1}{G_\rho^{-1} - [\hat{J}_{(\rho)}(0) + \hat{K}_{(\rho)}(0)]} = \frac{g_{\rho qq}^2}{m_\rho^2} \quad . \tag{5.36}$$

This procedure yields $g_{\rho qq}^2/4\pi = 1.05$. Then, the use of Eq. (5.35), with $\Lambda_\rho = 1.3$ GeV,

yields $g_{\rho NN}^2/4\pi = 2.48$, or $g_{\rho NN} = 5.58$. Finally, we obtain $f_{\rho NN} = 3.70 \, g_{\rho NN} = 20.6$,

which is quite close to the empirical value used in the OBE model. For example, in Ref. [7]

we see that $g_{\rho NN}^2/4\pi = 0.99$, or $g_{\rho NN}^{OBE} = 3.53$. Since the ratio $f_{\rho NN}^{OBE}/g_{\rho NN}^{OBE} = 6.1$, we have

$f_{\rho NN}^{OBE} = 21.5$, which is close to the value of $f_{\rho NN} = 20.6$ we have found for in our model

when $\kappa = 0.22$ GeV^2.

It should be noted that $G_\omega \neq G_\rho$ in our model, since $\hat{K}_{(\rho)}(q^2)$ is finite and $\hat{K}_{(\omega)}(q^2) = 0$

to a good approximation. Therefore, the success in obtaining good values for both

$g_{\omega NN}^2/4\pi$ and $f_{\rho NN}$ for the same value of κ is in part due to the importance of $\hat{K}_{(\rho)}(q^2)$ in this

analysis. We also remark that $g_{\rho NN}^2/4\pi \ll g_{\omega NN}^2/4\pi$ in the OBE model, since the first of these

- 22 -

values is close to 1 and the second is 20. Therefore, the fact that we overestimate $g_{\rho NN}^2 / 4\pi$ by about a factor of 2.5 (while obtaining a good value for $f_{\rho NN}$) may not be a particularly serious problem for our analysis.

VI. Discussion

It is generally understood that the longest range part of the nucleon-nucleon interaction is due to the exchange of the lightest meson in each channel. These mesons are described in the extended NJL model and we have seen that the bosonized model provides a good account of the nucleon-nucleon interaction for small momentum transfer. We also have the surprising result that the amplitude describing pion exchange is well described in our model over a broad range of momentum transfer. [See Fig. 10.] However, we do not know why our results for pion exchange at large $-q^2$ are so much better than our description of σ, ρ and ω exchange at large $-q^2$. It may be that the quark-quark T matrix is more adequately represented at large $-q^2$ in the case of the pion because of the pion's small mass. That is, higher-mass pseudoscalar mesons may be relatively less important than higher-mass mesons are in the other channels (ρ, σ, ω). It is possible that the consideration of the exchange of more massive mesons, or the calculation of more complex diagrams, will improve our results for the short-range aspects of the interaction.

We remark that another approach to the calculation of the nucleon-nucleon interaction is based upon baryon chiral perturbation theory [12]. That formalism does provide a good fit to the data; however, about 26 parameters are needed, including numerous contact interactions.

- 23 -

Such an analysis is presumably more fundamental than that based upon OBE models, which require the specification of about 10 parameters [7].

We may note that our work has provided a theoretical value for m_σ = 540 MeV. In the OBE model, m_σ is put equal to 550 MeV and the π, ρ and ω mesons are assigned their experimental mass. We have also provided reasonably successful calculations of $g_{\pi NN}$, $g_{\sigma NN}$, $g_{\omega NN}$ and $f_{\rho NN}$. However, there are still a number of additional parameters needed: Λ_ρ, Λ_π, Λ_ω, Λ_σ and $g_{\rho NN}$. We have seen how the empirical value of Λ_π may be understood in our model, when we take λ_π from a QCD-based calculation. Therefore, after adopting our theoretical results, there are still about four or five parameters that need to be specified when attempting to fit nucleon-nucleon scattering data using the OBE model. However, our analysis provides a significant reduction in the number of free parameters of that model.

References

[1]   Y. Nambu and G. Jona-Lasinio, Phys. Rev. $\underline{122}$, 345 (1961); $\underline{124}$, 246 (1961).

[2]   L.S. Celenza, C.M. Shakin, Wei-Dong Sun, J. Szweda, and Xiquan Zhu, Intl. J. Mod. Phys. E$\underline{2}$, 603 (1993).

[3]   L.S. Celenza, C.M. Shakin, Wei-Dong Sun, J. Szweda, and Xiquan Zhu, Ann. Phys. (N.Y.) $\underline{241}$, 1 (1995).

[4]   The construction of vertex operators for the confinement potential is discussed at length in L.S. Celenza, C.M. Shakin, Wei-Dong Sun, J. Szweda, and Xiquan Zhu, Phys. Rev. D$\underline{51}$, 3638 (1995).

[5]   Nan-Wei Cao, C.M. Shakin, and Wei-Dong Sun, Phys. Rev. C$\underline{46}$, 2535 (1992).

[6]   We find the momentum-space bosonization procedure of V. Bernard, A.A. Osipov and Ulf-G. Meissner, Phys. Lett. B$\underline{285}$, 119 (1992) to be particularly useful.

[7]   R. Machleidt, in Advances in Nuclear Physics, Vol. 19, eds. J.W. Negele and E. Vogt (Plenum, New York, 1989). (See Tables A.1 and A.2.)

[8]   C.M. Shakin, Wei-Dong Sun, and J. Szweda, Brooklyn College Report: BCCNT 95/051/246 (1995) − submitted to Physical Review C.

[9]   Keh-Fei Liu, Shao-Jing Dong, and Terrence Draper, Phys. Rev. Lett. $\underline{74}$, 2172 (1995). Here, the mass in the monopole form factor for the pion is found to be $\lambda_\pi = 0.75 \pm 0.14$ GeV.

[10]   L.S. Celenza, A. Rosenthal, and C.M. Shakin, Phys. Rev. C$\underline{31}$, 212 (1985).

[11]   Shun-fu Gao, C.M. Shakin, Wei-Dong Sun, and J. Szweda, Brooklyn College Report: BCCNT 95/071/248 (1995) − submitted to Physical Review C.

[12]   C. Ordonez, L. Ray and U. van Kolck, Phys. Rev. Lett. $\underline{72}$, 1982 (1994).

- 25 -

Acknowledgement

Table 1. Bosonization parameters for the omega meson, if the meson mass is fixed at $m_\omega = 0.783$ GeV and κ is varied. From OBE studies one has $g^2_{\omega NN}/4\pi = 20$ when $\Lambda^{OBE}_\omega = 1.5$ GeV [7]. (The theoretical value closest to the empirical value is found for $\kappa = 0.22$ GeV^2.)

κ (GeV^2)	G_ω (GeV^{-2})	$g_{\omega qq}$	$\dfrac{g^2_{\omega qq}}{4\pi}$	$\hat{J}_{(\omega)}(0)$ (GeV^2)	$\hat{J}_{(\omega)}(m^2_\omega)$ (GeV^2)	$\dfrac{g^2_{\omega NN}}{4\pi}$
0.16	7.10	3.39	0.917	0.0877	0.141	15.6
0.18	7.37	3.55	1.00	0.0872	0.136	17.1
0.20	7.62	3.71	1.10	0.0866	0.131	18.6
0.22	7.86	3.86	1.19	0.0861	0.127	20.2
0.24	8.08	4.01	1.28	0.0856	0.124	21.8
0.26	8.29	4.16	1.38	0.0852	0.121	23.4
0.28	8.49	4.31	1.48	0.0847	0.118	25.2

Fig. 1.   a.   The basic quark-loop integral of the NJL model is shown.

           b.   The function $\hat{J}_S(q^2)$ is defined by introducing a vertex (cross-hatched area) for the confining interaction V^C. See Ref. [10] for a detailed discussion of the construction of such vertex functions.

           c.   The function $K_S(q^2)$ is defined by the diagram shown. (See Ref. [9].)

           d.   The function $\hat{K}_S(q^2)$ is defined by including a vertex function for the confining interaction (cross-hatched region). (See Ref. [10].)

Fig. 2.   The function $J_P(t)$ is shown. Here $t = q^2$. The calculation is made by using a Euclidean momentum space with $\Lambda_E = 1.0$ GeV. Here $m_q = 0.262$ GeV and $G_S = 7.91$ GeV^{-2}.

Fig. 3.   a.   The diagram on the left is the basic quark loop integral of the NJL model. The propagators are $S_F(p) = (\not{p} - m_q + i\epsilon)^{-1}$, where m_q is the constituent quark mass. The additional diagrams show the introduction of a confining potential, V^C.

           b.   A vertex function for the confining interaction (cross-hatched area) is given by the equation shown [10].

           c.   Here the various terms summed in the equation depicted in (b) are shown.

Fig. 4.   The dashed line and the solid line for $t < 0$ denote the values of $J_S(t)$ calculated in a Euclidean momentum space with $\Lambda_E = 1.0$ GeV. The solid line for $t > 0$ represents the result of a calculation of $\hat{J}_S(t)$ in Minkowski space. There, a three-dimensional cutoff of $\Lambda_3 = 0.702$ GeV

is used for all the momentum vectors in the integral. We use $\kappa = 0.2 \text{ GeV}^2$, $m_q = 262 \text{ MeV}$, $G_S = 7.91 \text{ GeV}^{-2}$. Note that the inclusion of the confinement vertex function would hardly affect the result for $t < 0$.

Fig. 5.   The values of $\hat{J}_S(t)$ are shown for three values of κ.

a) $\kappa = 0.2 \text{ GeV}^2$,

b) $\kappa = 0.3 \text{ GeV}^2$,

c) $\kappa = 0.4 \text{ GeV}^2$.

The dotted line represents $1/G_S = 0.126 \text{ GeV}^2$ and the intersections with the solid lines represent the solution of the equation $1/G_S - \hat{J}_S(m_\sigma^2) = 0$.

Fig. 6.   The values of $\hat{J}_{(\omega)}(t)$ are shown for three values of κ.

a) $\kappa = 0.16 \text{ GeV}^2$,

b) $\kappa = 0.22 \text{ GeV}^2$,

c) $\kappa = 0.28 \text{ GeV}^2$.

The dotted line represents the value of $m_\omega^2 = (0.783 \text{ GeV})^2$. The intersections of the dotted line with the solid lines yields $1/G_\omega$ for the various values of κ. (See Table 1.)

Fig. 7.   The values of $\hat{J}_{(\rho)}(t) + \text{Re}\,\hat{K}_{(\rho)}(t)$ are shown for various κ.

a) $\kappa = 0.16 \text{ GeV}^2$,

b) $\kappa = 0.22 \text{ GeV}^2$,

c) $\kappa = 0.28 \text{ GeV}^2$.

The dotted line denotes the value of $m_\rho^2 = (0.770 \text{ GeV})^2$. The

intersection of the dotted line with the solid line yields the value of $1/G_\rho$.

Note that $\hat{J}_{(\rho)}(t) = \hat{J}_{(\omega)}(t)$. (From our study of omega exchange we have fixed $\kappa = 0.22$ GeV^2.)

Fig. 8.   Values of Re $\hat{K}_{(\rho)}(t)$ are shown for several values of κ.

  a) $\kappa = 0.16$ GeV^2,

  b) $\kappa = 0.22$ GeV^2,

  c) $\kappa = 0.28$ GeV^2.

Fig. 9.   (a)   The nucleon-nucleon interaction in the boson-exchange model is set equal to an interaction that is defined in terms of the quark-quark T matrix.

  (b)   Leading diagrams in $1/n_c$ are considered as discussed in Ref. [8].

  (c)   The T matrix t_{qq}, expressed in terms of the integrals $\hat{J}(t)$ and $\hat{K}(t)$ for the various channels, is used instead of the more general quark-quark T matrix of Fig. 9a to obtain the nucleon-nucleon interaction.

Fig. 10.   Values of $h_\pi^{NJL}(t)$ are given by the solid line and $h_\pi^{OBE}(t)$ is represented by the dotted line. Here $\lambda_\pi = 0.80$ GeV and $\Lambda_\pi^{OBE} = 1.3$ GeV. [See Eqs. (5.3), (5.6) and (5.8).]

$-iJ_S(q^2) = \cdots$ $q/2+k$ $\cdots\ q$ $-q/2+k$

(a)

$-i\hat{J}_S(q^2) = \cdots$ $q/2+k$ $\cdots\ q$ $-q/2+k$

(b)

$-iK_S(q^2) = \cdots$ π π $\cdots\ q$

(c)

$-i\hat{K}_S(q^2) = \cdots$ π π $\cdots\ q$

(d)

FIG. 1

FIG. 2

$J_p(t)$ (GeV^2)

t (GeV^2)

FIG.3

$J_S(t)$ and $\hat{J}_S(t)$ (GeV^2)

t (GeV^2)

FIG. 4

FIG. 5

FIG. 6

$\hat{J}_{(\rho)}(t) + Re \hat{K}_{(\rho)}(t)$ (GeV^2)

$t\,(GeV^2)$

a

b

c

FIG.7

$Re\hat{K}_{(\rho)}(t)$ (GeV^2)

$t\,(GeV^2)$

a

b

c

FIG. 8

FIG. 9

FIG. 10

Axis labels: $h_\pi^{OBE}(t)$ and $h_\pi^{NJL}(t)$ (vertical axis), $t\,(GeV^2)$ (horizontal axis)

Vertical axis values: 1.0, 0.8, 0.6, 0.4, 0.2, 0

Horizontal axis values: -2.0, -1.6, -1.2, -0.8, -0.4, 0